

January 2003

Prediction of entropy and dynamic properties of water below the homogeneous nucleation temperature

Francis W. Starr
Wesleyan University

C. A. Angell

H. E. Stanley

Follow this and additional works at: <http://wescholar.wesleyan.edu/div3facpubs>

 Part of the [Physics Commons](#)

Recommended Citation

Starr, Francis W.; Angell, C. A.; and Stanley, H. E., "Prediction of entropy and dynamic properties of water below the homogeneous nucleation temperature" (2003). *Division III Faculty Publications*. Paper 139.
<http://wescholar.wesleyan.edu/div3facpubs/139>

This Article is brought to you for free and open access by the Natural Sciences and Mathematics at WesScholar. It has been accepted for inclusion in Division III Faculty Publications by an authorized administrator of WesScholar. For more information, please contact dschnaidt@wesleyan.edu, ljohnson@wesleyan.edu.



ELSEVIER

Available online at www.sciencedirect.com

SCIENCE @ DIRECT®

Physica A 323 (2003) 51–66

PHYSICA A

www.elsevier.com/locate/physa

Prediction of entropy and dynamic properties of water below the homogeneous nucleation temperature

Francis W. Starr^{a,b,*}, C. Austen Angell^c, H. Eugene Stanley^a

^a*Center for Polymer Studies, Center for Computational Science, and Department of Physics, Boston University, Boston, MA 02215, USA*

^b*Polymers Division and Center for Theoretical and Computational, Materials Science, National Institute of Standards and Technology, Gaithersburg, MD 20899, USA*

^c*Department of Chemistry, Arizona State University, Tempe, AZ 85287, USA*

Received 29 November 2002

Abstract

The behavior of thermodynamic and dynamic properties of liquid water at atmospheric pressure in the temperature range between the lower limit of supercooling ($T_H \approx 235$ K) and the onset of the glassy state at T_g has been the focus of much research, and many questions remain about the properties of water in this region. Since direct measurements on water in this temperature range remain largely infeasible, we use existing experimental measurements of the entropy, specific heat, and enthalpy outside this range to construct a possible form of the entropy in the “difficult-to-probe” region. Assuming that the entropy is well-defined in extreme metastable states, and that there is no intervening discontinuity at atmospheric pressure, we estimate the excess entropy S_{ex} of the liquid over the crystal within relatively narrow limits. We find that our approximate form for S_{ex} shows atypical behavior when compared with other liquids: using a thermodynamic categorization of “strong” and “fragile” liquids, water appears to be fragile on initial cooling below the melting temperature, and strong in the temperature region near the glass transition. This thermodynamic construction can be used, with appropriate reservations, to estimate the behavior of the dynamic properties of water by means of the Adam–Gibbs equation—which relates configurational entropy S_{conf} to dynamic behavior. Although the Adam–Gibbs equation uses S_{conf} rather than S_{ex} as the control variable, the relation has been used successfully in a number of experimental studies with S_{conf} replaced by S_{ex} . This is likely a result of a proportionality between S_{conf} and S_{ex} , which we confirm for simulations of a model

* Corresponding author. Tel.: +1-301-975-8359; fax: +1-301-975-5012.

E-mail address: fstarr@nist.gov (F.W. Starr).

of water. Hence by using the constructed values of S_{ex} , together with experimental data in the range where S_{ex} is known, we estimate the temperature dependence of viscosity and diffusivity approaching the glass transition. Like the entropy plots, Arrhenius plots of viscosity or diffusion show an inflection, implying a crossover from fragile to strong liquid character below T_H . The dynamics results also imply $T_g \approx 160$ K, which is considerably above the expected value of 136 K from older experiments, but consistent with other recent evidence based on hyperquenched glass properties. We discuss the possibility of experimentally verifying our predictions, and briefly discuss other liquids that also may follow a strong-to-fragile pattern.

© 2003 Elsevier Science B.V. All rights reserved.

1. Introduction

In comparison with simple liquids, it is evident that there is a problem connecting the thermodynamic behavior of water at normal temperatures to that of “glassy” water found below a glass transition temperature T_g , typically believed to be 136 K [1,2], although recent evidence suggest T_g may be near 170 K [3]. One possibility is that the properties vary smoothly without a discontinuity [4–8]. A second possibility is that water near T_g and water near the melting temperature T_m belong to distinct phases, so that a phase transition must occur between them [2,9–11]. A third possibility is that there is no thermodynamically reversible path of any kind connecting the two states. To address these possibilities, Refs. [7,11] focused on a thermodynamically-plausible form for the entropy connecting the supercooled liquid and glassy states and determined the limits on the entropy of the glass that are compatible with the possibility of continuity. The entropy at 150 K, after annealing the sample, was subsequently measured [8] and found to be consistent with (but without requiring) thermodynamic continuity between the liquid near T_m and a possible liquid or glass at 150 K.

The dynamic properties of water along the $P = 0.1$ MPa isobar are also topic of continuing debate. For $T > T_H = 235$ K (the homogeneous nucleation temperature), the dynamic properties are those of a “fragile” liquid—namely highly non-Arrhenius temperature dependence. Indeed, in this T range, water appears to be one of the most fragile liquids studied. However, when glassy water is heated above the traditionally accepted $T_g = 136$ K, there is an increase in specific heat C_P that is both extremely small and broad, a characteristic of a very “strong” liquid; strong liquids exhibit low-temperature Arrhenius dependence, with activation energy $E \approx 14RT_g$. The specific heat behavior led to the conjecture that, for some $T < T_H$, water undergoes a crossover from fragile to strong behavior [12]. Subsequent experimental results have both supported [13] and disagreed [14] with the possibility of strong liquid behavior near T_g .

Crystallization at T_H on supercooling the liquid and at T_x on heating glassy water during normal time scale measurements might seem to make the above questions merely hypothetical, but the important fact is that liquid water may exist in this difficult-to-probe domain, and can be observed (in principle) if T is changed at some

rate that exceeds the “critical cooling rate” associated with crystal nucleation.¹ From a practical standpoint, such measurements are possible from hyperquenching experiments. A further possible complication is the ambiguity in the definition of entropy for metastable states [15]. We will present a detailed discussion of these complicating issues. Regardless of these complications, theoretical speculation about the region $T_x < T < T_H$ provides hypotheses that can be eventually tested. There are various approaches that can be taken, some of which will be discussed. Here we use thermodynamic reasoning to anticipate thermodynamic and dynamic properties.

In this paper we will address four specific issues: (i) assuming no thermodynamic transition at 0.1 MPa, what is the form of the entropy as a function of temperature in the difficult-to-probe region? (ii) How does the behavior of the entropy of water compare with that of other liquids? (iii) What implications could the form of the entropy have for dynamic properties? (iv) What evidence is there for and against strong behavior of dynamics properties from experiments, simulations, and from results on other network-forming fluids? To this end, we use experimental data on the specific heat, entropy, and enthalpy in both the liquid and glassy states to construct a possible form of the entropy in the difficult-to-probe region at 0.1 MPa.² We use the form for the entropy, in conjunction with the theory of Adam and Gibbs [17], to predict the behavior of the diffusion constant. Finally, we consider the results of recent simulations which begin to explore the experimentally difficult-to-probe domain.

Since conclusive experimental data in this region are unavailable, our results are offered as predictions to be confirmed or refuted by experiments. Our predictions are consistent with the observation of phenomena in related systems—such as SiO_2 and BeF_2 —that are comparable to those we discuss for water, but that appear under conditions of thermodynamic stability where they can be studied without interference from crystallization.

2. Excess entropy at atmospheric pressure

To illustrate the utility of thermodynamics in identifying the existence of a transition or other anomalous behavior of thermodynamic properties, consider a hypothetical situation in which we know the large differences in the enthalpy H , entropy S , and specific heat C_P of liquid water at 10°C and of ice Ih at -10°C , but are not aware of the first-order melting transition that lies between these temperatures. The only way to reconcile the large differences in H and S would be to hypothesize a discontinuity in S or a large “spike” in C_P in this temperature range which, in this case, we know arises

¹ The existence of liquid water at temperatures within this domain is demonstrated by the successful suppression of crystallization by the hyperquenching process introduced by Mayer and Dubochet, and later refined by Mayer. After a subsequent annealing process near T_g to relax out the high-energy state initially trapped during the quench, the properties of the glassy state of water produced by this process are essentially the same as those of the amorphous product obtained by the earlier method of cold substrate vapor deposition.

² The region $T_x < T < T_H$ is only “inaccessible” by ordinary time scale experiments. However, recent experiments have probed the liquid even at ordinary time scales by exploiting the equality of the Gibbs potential of the liquid and crystal along the metastable melting lines [16].

from a first-order melting transition. In this way, using only thermodynamic data, one can place limits on the thermodynamic behavior near the melting transition. Motivated by this consideration, we consider the changes in the supercooled liquid properties in the range $T_x < T < T_H$, where similar, though less dramatic, changes in thermodynamic properties have been measured.

To determine a reasonable form for the entropy $S=S(T,P)$ in this range, we first focus on thermodynamic properties that facilitate calculation of S in the easily-accessible regions $T > T_H$ and $T < T_x$, whose values also place strict limits on the possible behavior of S in the region $T_x < T < T_H$. First, we define the excess enthalpy

$$H_{\text{ex}} \equiv H_{\text{liquid}} - H_{\text{crystal}} , \quad (1a)$$

the difference of the liquid and crystal enthalpies, the excess entropy

$$S_{\text{ex}} \equiv S_{\text{liquid}} - S_{\text{crystal}} \quad (1b)$$

and the excess specific heat

$$C_P^{\text{ex}} \equiv C_P^{\text{liquid}} - C_P^{\text{crystal}} = T \left(\frac{\partial S_{\text{ex}}}{\partial T} \right)_P = \left(\frac{\partial H_{\text{ex}}}{\partial T} \right)_P . \quad (1c)$$

Each of these three quantities is known experimentally outside the difficult-to-probe region; in particular, we will use the values at the bounds of this region (tabulated in Table 1) to limit the possible forms of S_{ex} .

Consider these quantities in each of the temperature regions:

- The $T > T_H$ region: $H_{\text{ex}}(T_H)$ has been measured from the heat of crystallization of supercooled water [19]. We can relate measured values of C_P^{ex} to S_{ex} by integrating Eq. (1c),

$$S_{\text{ex}}(T) = S_{\text{ex}}(T_M) - \int_T^{T_M} \frac{C_P^{\text{ex}}}{T} dT, \quad (T < T_M), \quad (2)$$

where $S_{\text{ex}}(T_M)$ is the entropy of fusion. We numerically evaluate the integral in Eq. (2) for $T > T_H$, since we know C_P^{liquid} from recent bulk sample studies at temperatures from T_M down to -29°C [20] (and by emulsion studies down to -37°C [19]), and we know C_P^{crystal} for all $T < T_M$ [21].

- The $T < T_x$ region: $H_{\text{ex}}(T_x) = H_{\text{liquid}}(T_x) - H_{\text{crystal}}(T_x)$ has been measured from the heat of crystallization of glassy water.³ C_P^{ex} below T_x is known to be very small, and may be taken to be nearly T -independent for $T \approx T_x$. $S_{\text{ex}}(T_x)$ is known from the vapor pressure experiments on the glass and the crystal states [8].
- The “difficult-to-probe” $T_x < T < T_H$ region: We construct two possible forms for S_{ex} for $T_x < T < T_H$ similar to the methods of Refs. [7,11], but we now include

³ H_{ex} is measured by the heat released when freezing to the crystalline state. At 150 K, water freezes not to ice Ih, but to ice Ic with $H_{\text{ex}} = 1330$ J/mol. To account for the enthalpy difference between ice Ic and Ih, we also include 50 J/mol, the heat evolved when ice Ic transforms to ice Ih. See Ref. [23].

Table 1

Thermodynamic properties of water at 0.1 MPa at the homogeneous nucleation temperature T_H on cooling and the crystallization temperature T_x on heating

	$T_x = 150$ K	$T_H = 236$ K
C_P^{ex} (J/(K mol))	≈ 2 [6,7,18]	69.2 ± 0.5 [19–21]
S_{ex} (J/(K mol))	1.7 ± 1.7 [8]	15.2 ± 0.1 [19,21,22]
H_{ex} (J/mol)	1380 ± 20 [23]	4290 ± 20 [19,22]

Here, $Y_{\text{ex}} \equiv Y_{\text{liquid}} - Y_{\text{crystal}}$, the excess value of quantity Y of the liquid value relative to the ice Ih value. The uncertainties of S_{ex} and H_{ex} are taken from Ref. [22] which presents arguments supporting the reliability of the data.

the known value of $S_{\text{ex}}(T_x)$. To connect the regions $T > T_H$ and $T < T_x$, we must consider the thermodynamic constraints on the entropy. These constraints are:

- (i–iv) S_{ex} and C_P^{ex} fix the endpoints and the slopes of S_{ex} at T_x and T_H —four constraints.
- (v) $S(T)$ must be a monotonic increasing function because $C_P^{\text{ex}} \geq 0$. Note that this is not a uniquely defined constraint.
- (vi) The area A under the curve $S(T)$ is defined by the excess Gibbs free energy G_{ex} and is found using the experimental data of Table 1,

$$\begin{aligned}
 A &\equiv \int_{T_x}^{T_H} S_{\text{ex}} \, dT = G_{\text{ex}}(T_x) - G_{\text{ex}}(T_H) \\
 &= [TS_{\text{ex}} - H_{\text{ex}}]_{T_x}^{T_H} = 422 \pm 30 \text{ J/mol} .
 \end{aligned} \tag{3}$$

Our challenge is to determine a functional form for $S_{\text{ex}}(T)$, given only its values at the limiting temperatures T_x and T_H , the area A under $S(T)$, and the monotonicity of $S(T)$. Three possible choices include:

- (i) A discontinuity in $S_{\text{ex}}(T)$ itself, (i.e., a first-order phase transition).
- (ii) A kink in $S(T)$, which would imply a discontinuity in C_P^{ex} (i.e., a second-order phase transition) or a divergence in C_P , or a λ -transition (as in sulfur).
- (iii) A simple inflection in $S(T)$, which implies a maximum in C_P^{ex} (i.e., a no-transition or a transition of order larger than two).

The available data cannot distinguish among these three possibilities. However, experimental [16] and simulation [24] results suggest that, if there is a first-order transition (option (i)), it occurs only at a pressure $P \geq 100$ MPa, suggesting that at 0.1 MPa option (iii) is the most likely. We therefore focus on developing a plausible form for $S(T)$ such that C_P^{ex} is not singular, although we cannot rule out option (ii).

To illustrate two possible forms of S_{ex} , we take a simple approach and use a high-order polynomial that satisfies all constraints. The six constraints cannot generally be satisfied by a polynomial of only order five, because the monotonicity of $S_{\text{ex}}(T)$ requires the slope to be positive at all points; additionally, this requirement does not

yield a unique solution. We are able to satisfy all constraints (but not uniquely) using a seventh-order polynomial form

$$S_{\text{ex}}(T) = \sum_{n=0}^7 a_n T^n. \quad (4)$$

We show a possible choice of coefficients for the case using the upper and lower bounds on the area constraint of S_{ex} in Fig. 1. These two curves represent approximate bounds on the form of S_{ex} in the unknown region; these bounds are somewhat larger if the uncertainty in S_{ex} , particularly at T_x , is also included.

While there are an infinite number of possible forms depending on precise parameter choices, all such choices give forms of S_{ex} that lie near the approximate bounds indicated in Fig. 1. From a physical standpoint, all of these forms are qualitatively very similar, and so any conclusions we draw from this analysis are unlikely to be affected by the exact parameter choices. Fig. 1 shows that S_{ex} and C_P^{ex} both show significant changes in their behavior below 230 K. This is a result of the fact that S_{ex} must remain nearly constant near T_x in order to satisfy the constraint of Eq. (3); hence, as S_{ex} approaches T_H , a less pronounced change than shown in Fig. 1(a) would bound an area $\int_{T_x}^{T_H} S_{\text{ex}} dT$ larger than 422 ± 30 J/mol. Furthermore, the inflection in S_{ex}

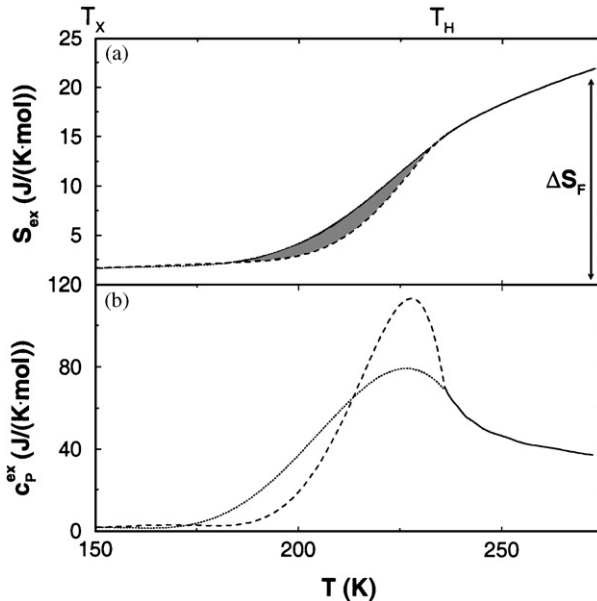


Fig. 1. (a) Possible forms for the excess entropy S_{ex} in the experimentally inaccessible region. The two curves show the fits obtained using the upper and lower bounds on the area under S_{ex} , given Eq. (3). Any thermodynamically plausible form of S_{ex} (without a discontinuity) can vary only slightly from these “bounding” forms (due to the uncertainty in H_{ex}). The entropy of fusion $\Delta S_F = 21.8$ J/(K mol) for freezing at 273 K is indicated by the arrow. (b) Constant pressure excess specific heat $C_P^{\text{ex}} = T(dS_{\text{ex}}/dT)_P$ for the possible forms of S_{ex} shown in (a).

(Fig. 1) must occur at $T \geq 215$ K, since, were the inflection to occur at a significantly lower temperature, the area A would also be too large.

The behavior of S_{ex} for water is qualitatively distinct from the behavior of S_{ex} for the majority of other liquids (at least of liquids for which the necessary thermodynamic data are available). To illustrate this point, we present experimental data in a fashion reminiscent of the “strong/fragile pattern” of viscosity behavior. The presentation requires knowledge of the excess entropy of the liquid compared to the crystal at T_g , which is used for scaling purposes, and at temperatures above it. From the fits in Fig. 1, we calculate $S_{ex}(T_g) = 1.5$ J/(K mol) using a constant value of $C_P^{ex} = 2$ J/(K mol) and integrating from 150 K “down” to the traditionally assigned $T_g = 136$ K. (We emphasize that the exact numerical choice of T_g here does not affect our qualitative results, since we will later see our data supports a higher value of T_g .) We then plot S_{ex} scaled by T_g and compare the behavior of water with that of a wide variety of other liquids covering a broad range of fragilities (Fig. 2); it is clear that the behavior of water must be an extreme case of liquid behavior.

As a further consideration, we focus on the fact that ice, unlike most simple crystals, has a residual entropy S_{res} due to proton disorder estimated by $S_{res} = R \ln(3/2) = 3.4$ J/(K mol) [25]. As a result, when we compute the difference $S_{ex} \equiv S_{liquid} - S_{crystal}$, we are also removing S_{res} from S_{liquid} . To compare more clearly with other liquids, we should restore this residual component, since we expect it is a part of the entropy in the glass at T_g , so we also plot $[S_{ex}(T_g) + S_{res}(T_g)]/[S_{ex} + S_{res}]$ in Fig. 2, and find an even more dramatic departure from the typical liquid pattern. Whether or not the

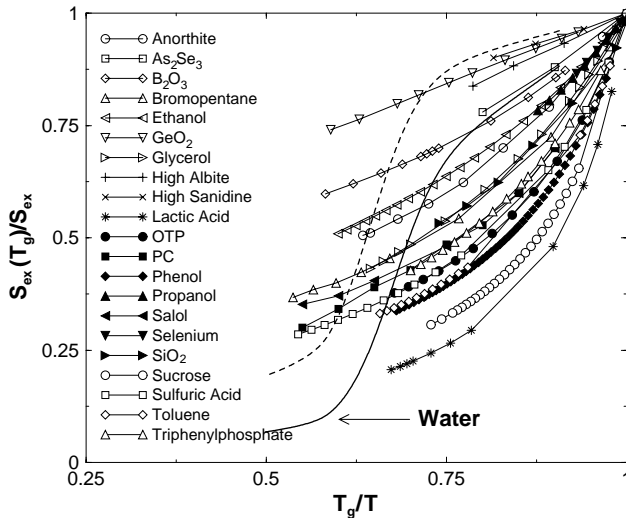


Fig. 2. “Thermodynamic fragility” measured by $S_{ex}(T_g)/S_{ex}$ for a wide variety of glass forming liquids in comparison with the predicted approximate form for water, taken as the average of the two extreme forms in Fig. 1. The solid curve is S_{ex} as normally calculated. The dashed curve is $S_{ex} + S_{res}$, which we expect is more relevant to glassy water, as discussed in the text. Non-water data are taken from Ref. [12].

residual entropy is included in the comparison, water near T_g is a very strong liquid by this thermodynamic classification scheme, perhaps the strongest, while near T_m , it is extremely fragile. This qualitative conclusion is unaffected by whether or not T_g is assigned the value 136 K or 165 K, as suggested by Velikov et al. [3]; using the higher value of T_g merely shifts the crossover to a larger value of T_g/T .

3. Possible consequences for dynamic behavior

We have seen from the behavior of S_{ex} in Fig. 2 that the behavior of water is unusual, thermodynamically resembling that of a strong liquid as we approach T_g . We now consider the possible implications of this approximate form for S_{ex} on the dynamic behavior of water below T_H , keeping in mind that these properties are, in principle, measurable. The entropy-based Adam–Gibbs theory [17] has been used to describe the relaxation of liquids approaching their glass transitions [26], and provides an explanation for the variation of diffusion constant D (even in anomalous cases, like SiO_2) and, by implication, the viscosity η [27–30]. We use the prediction

$$\eta = \eta_0 \exp\left(\frac{A}{TS_{\text{conf}}}\right), \quad (5)$$

where A is a constant.⁴ The configurational entropy of the liquid,

$$S_{\text{conf}} \equiv S_{\text{liquid}} - S_{\text{vib}}, \quad (6)$$

is the entropy arising from the degeneracy of the basins the liquid can sample in the energy landscape picture [31–33]. The vibrational component S_{vib} of the entropy is attributable to the thermal excitation the liquid experiences in the basin sampled.

Eq. (5) has been directly tested and confirmed in several recent simulations [28–30], including simulation of water [28]. Unfortunately, it is not possible to obtain S_{conf} without full knowledge of the vibrational entropy of the liquid, which is not experimentally accessible. For experimental tests of the Adam–Gibbs equation, the approximation $S_{\text{vib}} = S_{\text{crystal}}$ has been frequently employed; the approximation assumes that the shapes of the liquid and crystalline basins are identical, which one generally does not expect. Nonetheless, transport data, such as viscosity and dielectric relaxation time, have been linearized over many orders of magnitude using S_{ex} in Eq. (5). This success is paradoxical unless $S_{\text{vib}} \propto S_{\text{crystal}}$ —in other words, S_{vib} need not equal S_{crystal} if they are proportional, since this proportionality can be absorbed into the free fitting parameters [34]. There are several cases where data are available and such proportionality is found, including experiments on selenium and simple two-state models of

⁴ The Vogel–Fulcher–Tammann form $\eta = \eta_0 \exp(B/(T - T_0))$ for the temperature dependence of viscosity and characteristic times of liquids at low temperature can be obtained from Eq. (5) by assuming that $C_p^{\text{ex}} \propto T^{-1}$. Note that $T_0 < T_g$ is typically associated with an underlying “ideal” glass transition.

configurational excitation in Ref. [35]. In the next section, we also show results for a model of water which shows approximate proportionality. Hence, for many liquids, S_{ex} can be used in Eq. (5).

In the case of water, we expect the residual entropy S_{res} to be configurational, since it derives from the multiplicity of possible proton orientations; therefore S_{res} is involved in the reorientation of molecules within the hydrogen bond quasi-lattice. As a result, we must include S_{res} to correctly estimate S_{conf} . Hence we approximate

$$S_{\text{conf}} \approx S_{\text{ex}} + S_{\text{res}} . \quad (7)$$

Equivalently, this implies $S_{\text{vib}} = S_{\text{crystal}} - S_{\text{res}}$, i.e., S_{res} should not contribute to the vibrational entropy. We substitute Eq. (7) in Eq. (5) to predict the behavior of η and D ⁵ for $T \leq T_H$.

We select parameters⁶ in Eq. (5) to fit S_{conf} to η [37] and D [38]⁷ (Fig. 3) for $T > 235$ K, where experimental measures of all quantities are available. The quality of fit in the regime where experimental data are available is shown in the inset of Fig. 3. The super-Arrhenius behavior for $T \geq 230$ K is reflected by the inflection of η and D ; this change is not clearly evident in η or D until $T \leq 190$, where the dynamic properties are approximately Arrhenius. In contrast to the fragile behavior for T close to T_H , the behavior for T near T_x is characteristic of a strong liquid [32]—Arrhenius behavior with an appropriate activation energy. Here, we find activation energy $E \approx 74$ kJ/mol, which converts to a “fragility index” $m = E/2.303RT_g = 28$ if we use $T_g = 136$ K, or $m = 24$ if we use $T_g = 160$ K, comparable to m for sodium trisilicate, a very strong liquid [39]. The value of E obtained agrees with that obtained experimentally by a standard analysis of the crystallization kinetics of vitreous water due to Haage et al. [40] who reported the value 67 kJ/mol. Comparable values are reported by Smith et al. [41] (84 kJ/mol) and Benniskens and Blake [42] (55 kJ/mol). The temperature dependence of the Avrami crystallization equation kinetic constant is expected to correspond to that of the viscosity of the crystallizing phase. However, Ngai et al. [43] point out that the temperature dependence is more correctly thought of as that of the diffusivity of the crystallizing phase, and show data for several molecular liquids in which the value is somewhat less than that expected from the Stokes–Einstein equation. These crystallization kinetics-based results are in conflict with the evaporation-rate based diffusivity results of Ref. [14], indicating that the behavior of water near T_x remains fragile with

⁵ We make predictions for both η and D . However, the decoupling of D from η —evidenced by the breakdown of the Stokes–Einstein relationship at low T —means that our predictions for D may not be accurate. The decoupling might be associated with a “normal” component of D that is not strongly affected by the dramatic increases in η , such as sometimes observed near critical point [36].

⁶ For the diffusion, we use $D_0 = 1.08 \times 10^{-3}$ cm²/s and $A = -31.6$ kJ/mol. For the viscosity, we use $\eta_0 = 1.64 \times 10^{-4}$ P and $A = 31.9$ kJ/mol. These parameters were obtained by fitting S_{conf} to the experimental data in the region between $T = 235$ and 273 K.

⁷ The values of D reported in Ref. [38] are $\approx 7\%$ too small. Increasing the measured D values by 7 would not change any conclusions presented here, and would also be indistinguishable on the scale of Fig. 3(a) [38].

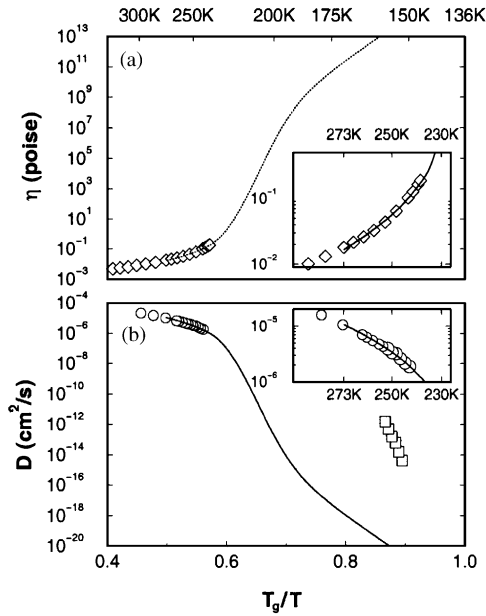


Fig. 3. (a) Fit of S_{ex} and viscosity η using Eq. (5). Experimental data (\diamond) are from Ref. [37]. Diffusion constant D predicted using the same method. The experimental data (\circ) for $T > 235$ K are from Ref. [38]. The data for $T < 160$ K (\square) are from Ref. [14]. (b) Both (a) and (b) show behavior expected for a strong liquid for $T \leq 220$ K—i.e., Arrhenius behavior with an activation energy $\approx T_g/3$ (in units of kJ/mol) [32]. The insets show the quality of the fit in the region where experimental data are available.

an activation energy of ≈ 170 kJ/mol. A crossover from fragile to strong behavior is not typical of liquids, but does appear in simulations of BeF_2 and SiO_2 [30,44]. The large number of conflicting results on this question demonstrates the need for further experimental scrutiny.

4. Simulation evidence

Computer simulations also offer an opportunity to explore the possible change in dynamic properties on cooling. Simulations of the SPC/E model [45,46] of water show a power law (similar to that observed experimentally) which has been interpreted in the framework of mode coupling theory (MCT) [47]. More importantly, just below the MCT transition temperature, the power-law behavior crosses over to Arrhenius-type behavior with the activation energy characteristic of a strong liquid (Fig. 4) initially reported in Ref. [46] for the isochoric path. Note that no inflection is apparent in Fig. 4(a) along the isochoric path, due in part to the fact that the properties change less dramatically along paths of constant density. Results for the same model along an *isobaric* path (such as that studied experimentally), suggest a slight inflection in D

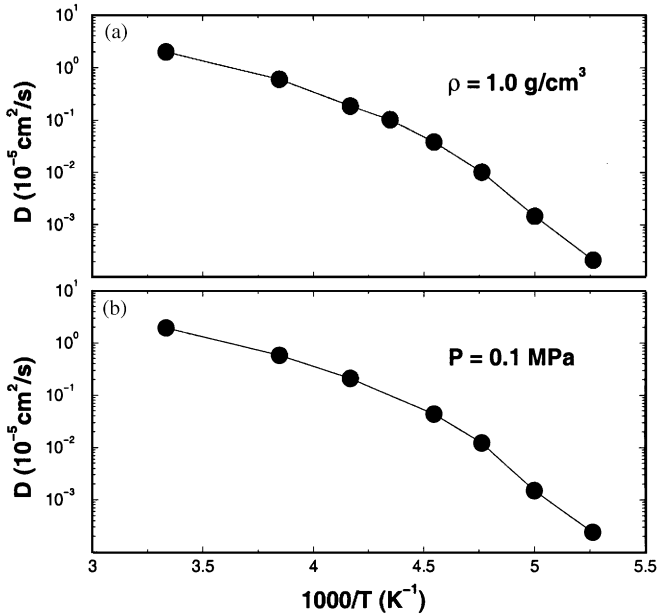


Fig. 4. Diffusion constant D calculated from simulations of the SPC/E model in Ref. [46] along (a) an isochoric path and (b) an isobaric path. No inflection is apparent along the isochoric path, but a weak inflection occurs along the isobaric path; a stronger inflection is expected in water along the path of atmospheric pressure.

(Fig. 4(b)). This inflection is at least in part a result of the fact that more significant structural changes occur along an isobaric path, since density is allowed to vary. That the inflection is far less pronounced than our predictions based on experimental data is consistent with the fact that the SPC/E potential tends to exhibit less dramatic anomalies than observed experimentally (such as the density maximum) [48].

We also show S_{conf} evaluated exactly for the SPC/E model (Fig. 5). Details of the calculations and the original simulated data can be found in Ref. [28], which verified the validity of the Adam–Gibbs expression for the potential. The only difference in the present calculation and that of Ref. [28] is that we include data for one lower temperature ($T = 180 \text{ K}$), and we do not assume a $T^{3/5}$ dependence of the potential energy, which would preclude any inflection in S_{conf} . Instead, we use a spline function when fitting the potential energy that can accommodate the slight inflection that becomes more obvious at the lowest temperatures. Consistent with the crossover in dynamic properties just below T_{MCT} , S_{conf} has a weak inflection leading to a much slower decrease with T . Similar results have recently been found for silica [30], with a more pronounced inflection.

To justify the use of S_{ex} for the experimental data, we also show S_{ex} evaluated for the SPC/E model (Fig. 5). Details of the ice simulation are given in Ref. [49]. In the inset, we have made a parametric plot of S_{conf} and S_{ex} , demonstrating the linear

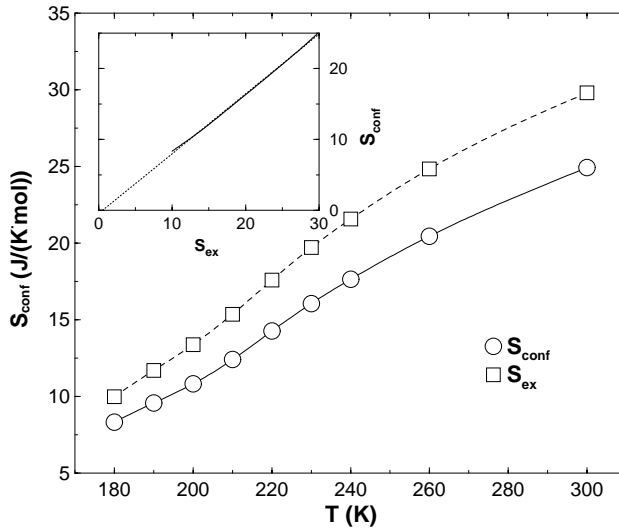


Fig. 5. Exact evaluation of S_{conf} for the SPC/E model showing a weak inflection at lowest temperatures for which simulations are feasible. We also show S_{ex} for the same model. The inset shows a parametric plot (solid line) to demonstrate proportionality; the dotted line is the best fit line to the results, which intercepts the y -axis at -0.43 —only slightly below the ideally expected value of zero.

proportionality. Such proportionality is required if S_{ex} can be expected to linearize dynamic data.

5. Discussion

The behavior of the entropy, the quantity estimated most directly from the available experimental data, establishes that water differs from most other liquids. The use of the estimated S_{conf} in the Adam–Gibbs equation is more speculative, but the results obtained may be experimentally significant, as we will discuss.

There are at least two other liquids, BeF_2 and SiO_2 , that show similar characteristics to those reported in Figs. 1 and 3, with the primary difference that these characteristics are only manifested at much higher temperatures relative to both glass temperatures and melting points [30,44]. Both of these liquids exhibit pronounced maxima in their heat capacities and show associated anomalies in their viscosities; preliminary data are available in Ref. [30,44]. Both substances have a tetrahedral network structure, though differ by having bridges between the network centers that are large, relative to the protons of water. Hence the behavior reported here may be characteristic of a much broader class of liquids.

The behavior of η observed in Fig. 3(a) raises another interesting possibility; for most systems the value of $\eta(T_g) \approx 10^{13}$ P, while Fig. 3(a) shows that η reaches this value at $T \approx 160$ K, significantly higher than the expected $T_g = 136$ K. This may be an

indication of the limitations of our approach to estimating the dynamic properties, both because we do not have direct access to S_{conf} and so must estimate it crudely from S_{ex} , and because the range of T where experimental measures of η are available to estimate parameters for the Adam–Gibbs expression. The difference in T_g values could possibly reflect a weakness in using the Adam–Gibbs expression itself; however, this appears less likely given the recent success of computer simulations where S_{conf} may be directly calculated. Alternatively, this may be an indication that T_g of water is, in fact, significantly larger than 136 K. Velikov et al. [3] show that the thermal data for hyper-quenched glassy water are incompatible with what is known about the relaxation of trapped enthalpy from other hyper-quenched glasses, and that the incompatibility can only be resolved if the data for water are re-scaled using a glass transition temperature of 165–170 K. This roughly coincides with the T_g predicted by Fig. 3. However, if this were the case, the data used at $T = 150$ K would be for the glassy state, and hence $S_{\text{ex}}(150 \text{ K})$ would be smaller for the entropy that would be measured for an equilibrium state. The uncertainty in the entropy associated with passing through the glass transition at different rates has been carefully assessed by Goldstein [50] and found to be small for the range of rates examined. In many cases, this ambiguity can be removed by relaxing the frozen structure at $T < T_x$. Even if equilibrium is not reached, it would not seriously effect our estimates because the value of $S_{\text{ex}}(150 \text{ K})$ is already extremely small and further relaxation would only reduce it closer to zero; this would result in a slightly more pronounced inflection on S_{ex} than we have anticipated here, and so we do not expect possible non-equilibrium effects to alter our qualitative conclusions.

Other supporting evidence pointing to a higher T_g value may be available from experiments on the nano-droplets of water that occur in “hydrogels”. These are heavily hydrated hydrophilic polymers e.g., polyhydroxy ethyl-methacrylate. In the thermal studies of such media by Hofer et al. [51], a glass transition temperature of 162 K was observed, independent of the water content over a considerable range of water contents. When freezing of the water was induced by thermal cycles in these systems, the glass transition at 162 K disappears from the thermal analysis traces. Its origin was somewhat ambiguous since the authors referred to a weaker feature of the traces, seen at 136 K, as the glass transition for water. Joining this fact with the present results with the aforementioned hyper-quenching results, it seems plausible that a $T_g = 162$ K glass transition might be appropriate to bulk water. However, such a possibility remains speculative at this time. A more detailed discussion of this matter is given in a recent review [52].

We also comment on the apparent crossover of the dynamic properties from fragile to a strong liquid behavior. In the experiments reported in Ref. [51], the activation energy for the thermal relaxation lies in the range 80–120 kJ/mol and a more detailed study of the relaxation that included annealing studies analyzed by the Tool–Narayanaswamy–Moyinhan phenomenological model [52], gave best fits to the data when an activation energy between the two above was used. These values are comparable with the slope in Fig. 3.

What are the prospects for providing experimental tests of the suggested behavior in the difficult-to-probe region? Probe molecule experiments that signal matrix dynamics

during rapid temperature changes are conceivable. So also are analyses of shapes of droplets splatted onto cold surfaces [53] in terms of viscosity-temperature-time histories. Another possibility is to study the properties of vitrified water as a function of the cooling rate, since it is now possible to achieve extremely high cooling rates [53]. The energy of the glassy state of water trapped during such a fast quench of the liquid is reflected directly in the annealing exotherm—the release of heat observed in any subsequent annealing process [3,23].

Based on relations between quench rates and relaxation times, an ergodic heat capacity can typically be determined for measurements made on a time scale of 10^{-5} s (or shorter) during a quench. These measurements can be carried out at temperatures down to the quench rate dependent fictive temperature, which has been estimated by Fleissner et al. [54] to be 200–230 K for hyperquenched water. If this is the case then during the quench, the liquid maintains its internally equilibrated condition from 5–35 K below the usual homogeneous nucleation temperature. Below this temperature, some ambiguity enters in the entropy determination due to the irreversibility that enters during ergodicity-breaking.

We conclude that water is a liquid in which there is a striking change in character as the temperature is changed between the melting point and the glassy state regime. The exact quantitative nature of this change is likely to remain a topic research for years to come.

Acknowledgements

We thank R.J. Speedy for his invaluable contributions. We also thank B.D. Kay, C.T. Moynihan, P.H. Poole, S. Sastry, F. Sciortino, and R.S. Smith for enlightening discussions. CAA acknowledges support from a NSF Solid State Chemistry grant DMR 9108028-002. The Center for Polymer Studies is supported by NSF grant CHE-0096892.

References

- [1] P.G. Debenedetti, *Metastable Liquids*, Princeton University Press, Princeton, NJ, 1996.
- [2] C.A. Angell, E.J. Sare, *J. Chem. Phys.* 52 (1970) 1058.
- [3] V. Velikov, S. Borick, C.A. Angell, *Science* 294 (2001) 2335.
- [4] C.G. Venkatesh, S.A. Rice, A.H. Narten, *Science* 186 (1975) 927;
S.A. Rice, M.S. Bergren, L. Swingle, *Chem. Phys. Lett.* 59 (1978) 14;
C.A. Angell, J.C. Tucker, *J. Phys. Chem.* 84 (1980) 268;
G.P. Johari, *J. Chem. Phys.* 105 (1996) 7079.
- [5] C.A. Angell, J. Shuppert, J.C. Tucker, *J. Phys. Chem.* 77 (1973) 3092.
- [6] G.P. Johari, A. Hallbrucker, E. Mayer, *Nature* 330 (1987) 552;
A. Hallbrucker, E. Mayer, G.P. Johari, *J. Phys. Chem.* 93 (1989) 4986.
- [7] G.P. Johari, G. Fleissner, A. Hallbrucker, E. Mayer, *J. Phys. Chem.* 98 (1994) 4719.
- [8] R.J. Speedy, P.G. Debenedetti, R.S. Smith, C. Huang, B.D. Kay, *J. Chem. Phys.* 105 (1996) 240.
- [9] R.J. Speedy, C.A. Angell, *J. Chem. Phys.* 65 (1976) 851;
R.J. Speedy, *J. Phys. Chem.* 86 (1982) 892.
- [10] M. Sugasaki, H. Suga, S. Seki, *Bull. Chem. Soc. Japan* 41 (1968) 2591;
G.P. Johari, *Philos. Mag.* 35 (1977) 1077.
- [11] R.J. Speedy, *J. Phys. Chem.* 96 (1992) 2232.

- [12] C.A. Angell, *J. Phys. Chem.* 97 (1993) 6339;
K. Ito, C.T. Moynihan, C.A. Angell, *Nature* 398 (1999) 492.
- [13] R. Bergman, J. Swenson, *Nature* 403 (2000) 283.
- [14] R.S. Smith, B.D. Kay, *Nature* 398 (1999) 788.
- [15] D.J. Evans, D.J. Searles, E. Mittag, *Phys. Rev. E* 63 (2001) 51 105;
F. Zhang, D.J. Isbister, D.J. Evans, *Phys. Rev. E* 64 (2001) 21 102.
- [16] O. Mishima, H.E. Stanley, *Nature* 392 (1998) 192;
O. Mishima, *Phys. Rev. Lett.* 85 (2000) 334.
- [17] G. Adam, J.H. Gibbs, *J. Chem. Phys.* 43 (1965) 139.
- [18] Y.P. Handa, D.D. Klug, *J. Phys. Chem.* 92 (1988) 3323.
- [19] C.A. Angell, M. Oguni, W.J. Sichina, *J. Phys. Chem.* 86 (1982) 998.
- [20] E. Tombari, C. Ferrari, G. Salvetti, *Chem. Phys. Lett.* 300 (1999) 749.
- [21] W.F. Giaque, J.W. Stout, *J. Am. Chem. Soc.* 58 (1936) 1144.
- [22] R.J. Speedy, *J. Phys. Chem.* 91 (1987) 3354.
- [23] P.Y. Harta, D.D. Klug, E. Whalley, *J. Chem. Phys.* 84 (1976) 7009;
A. Hallbrucker, E. Mayer, *J. Phys. Chem.* 91 (1987) 503.
- [24] P.H. Poole, F. Sciortino, U. Essmann, H.E. Stanley, *Nature* 360 (1992) 324;
S. Harrington, R. Zhang, P.H. Poole, F. Sciortino, H.E. Stanley, *Phys. Rev. Lett.* 78 (1997) 2409;
F. Sciortino, P.H. Poole, U. Essmann, H.E. Stanley, *Phys. Rev. E* 55 (1997) 727;
A. Scala, F.W. Starr, E. La Nave, H.E. Stanley, F. Sciortino, *Phys. Rev. E* 62 (2000) 8016.
- [25] L. Pauling, *J. Am. Chem. Soc.* 57 (1935) 2680.
- [26] J.H. McGill, *J. Chem. Phys.* 47 (1967) 2802;
G.W. Scherer, *J. Am. Ceram. Soc.* 67 (1984) 504;
C.A. Angell, *J. Res. NIST* 102 (1997) 171.
- [27] C.A. Angell, E.D. Finch, L.A. Woolf, P. Bach, *J. Chem. Phys.* 65 (1976) 3063.
- [28] A. Scala, F.W. Starr, E. La Nave, F. Sciortino, H.E. Stanley, *Nature* 406 (2000) 166.
- [29] S. Sastry, *Phys. Rev. Lett.* 85 (2000) 590.
- [30] I. Saika-Voivod, P.H. Poole, F. Sciortino, *Nature* 412 (2001) 514.
- [31] M. Goldstein, *J. Chem. Phys.* 51 (1969) 3728.
- [32] C.A. Angell, *Science* 267 (1995) 1924;
F.H. Stillinger, *Science* 267 (1995) 1935.
- [33] P.G. Debenedetti, F.H. Stillinger, *Nature* 410 (2001) 259.
- [34] L.M. Martinez, C.A. Angell, *Nature* 410 (2001) 663.
- [35] C.A. Angell, S. Borick, *J. Non-Cryst. Solids* 307–310 (2002) 393.
- [36] J.C. Allegra, A. Stein, G.F. Allen, *J. Chem. Phys.* 55 (1971) 1716.
- [37] J. Hallett, *Proc. Phys. Soc.* 82 (1963) 1046;
Yu.A. Osipov, B.V. Zheleznyi, N.F. Bondarenko, *Zh. Fiz. Khim.* 51 (1977) 1264.
- [38] K.T. Gillen, D.C. Douglass, M.J.R. Hoch, *J. Chem. Phys.* 57 (1972) 5117.
- [39] R. Bohmer, K.L. Ngai, C.A. Angell, D.J. Plazek, *J. Chem. Phys.* 99 (1993) 4201.
- [40] W. Haage, A. Hallbrucker, E. Mayer, G.P. Johari, *J. Chem. Phys.* 100 (1994) 2743.
- [41] R.S. Smith, C. Huang, E.K.L. Wong, B.D. Kay, *Surf. Sci. Lett.* 367 (1996) L13.
- [42] P. Jenniskens, D.F. Blake, *Astrophys. J.* 473 (1996) 1104.
- [43] K.L. Ngai, J.H. Magill, D.J. Plazek, *J. Chem. Phys.* 112 (2000) 1887.
- [44] M. Hemmati, C.T. Moynihan, C.A. Angell, *J. Chem. Phys.* 115 (2001) 6663;
C.A. Angell, R.D. Bressel, M. Hemmatti, E.J. Sare, J.C. Tucker, *Phys. Chem. Chem. Phys.* 2 (2000) 1599.
- [45] P. Gallo, F. Sciortino, P. Tartaglia, S.-H. Chen, *Phys. Rev. Lett.* 76 (1996) 2730;
F. Sciortino, P. Gallo, P. Tartaglia, S.-H. Chen, *Phys. Rev. E* 54 (1996) 6331;
F. Sciortino, L. Fabbian, S.-H. Chen, P. Tartaglia, *Phys. Rev. E* 54 (1997) 5397;
F.W. Starr, S. Harrington, F. Sciortino, H.E. Stanley, *Phys. Rev. Lett.* 82 (1999) 3629.
- [46] F.W. Starr, F. Sciortino, H.E. Stanley, *Phys. Rev. E* 60 (1999) 6757.
- [47] W. Götze, L. Sjögren, *Rep. Prog. Phys.* 55 (1992) 241.
- [48] S. Harrington, P.H. Poole, F. Sciortino, H.E. Stanley, *J. Chem. Phys.* 107 (1997) 7443.
- [49] F.W. Starr, S. Sastry, E. La Nave, A. Scala, H.E. Stanley, F. Sciortino, *Phys. Rev. E* 63 (2001) 041201.

- [50] M. Goldstein, *J. Chem. Phys.* 64 (1976) 4767.
- [51] K. Hofer, E. Mayer, G.P. Johari, *J. Phys. Chem.* 94 (1990) 2689;
K. Hofer, E. Mayer, I.M. Hodge, *J. Non-Cryst. Solids* 139 (1992) 78;
K. Hofer, E. Mayer, G.P. Johari, *J. Phys. Chem.* 95 (1991) 7100.
- [52] C.T. Moynihan, et al., *J. A., Ann. NY Acad. Sci.* 279 (1976) 15;
C.A. Angell, *Chem. Rev.* 102 (2002) 2627.
- [53] E. Mayer, *J. Appl. Phys.* 58 (1985) 663;
E. Mayer, *J. Microsc.* 140 (1985) 3;
E. Mayer, *J. Microscop.* 141 (1986) 269.
- [54] G. Fleissner, A. Hallbrucker, E. Mayer, *J. Phys. Chem. B* 102 (1998) 6239.